

Gradient-free training of autoencoders for non-differentiable communication channels

Ognjen Jovanovic, *Student Member, IEEE*, Metodi Yankov, *Member, IEEE*, Francesco Da Ros, *Senior Member, IEEE*, and Darko Zibar, *Member, IEEE*

Abstract—Training of autoencoders using the backpropagation algorithm is challenging for non-differentiable channel models or in an experimental environment where gradients cannot be computed. In this paper, we study a gradient-free training method based on the cubature Kalman filter. To numerically investigate the method, the autoencoder is employed to perform geometric constellation shaping on a non-differentiable communication channel that includes: laser phase noise, additive white Gaussian noise and blind phase search-based phase noise compensation. Our results indicate that the autoencoder can be successfully optimized using the proposed training method. We also show that the learned constellations are more robust to residual phase noise with respect to standard constellation schemes such as Quadrature Amplitude Modulation and Iterative Polar Modulation for the considered conditions.

Index Terms—Optical fiber communication, cubature Kalman filter, end-to-end learning, geometric constellation shaping, phase noise.

I. INTRODUCTION

COMMUNICATION systems with high spectral efficiency are critical to meet future data traffic requirements [1]. Such systems with uniformly distributed signalling (such as conventional quadrature amplitude modulation (QAM)) suffer from a gap to the theoretically achievable information rate, which can be closed by constellation shaping. In particular, geometric constellation shaping (GCS) is the process of optimizing the positions of the constellation points on the I/Q plane. In [2], this optimization is performed in an end-to-end manner by embedding a differentiable channel model in an autoencoder (AE) framework. The approach can be utilized for coherent fiber optic communication to e.g. learn geometric constellation shapes which are jointly robust to amplification noise and signal dependent nonlinear effects in multi-span links [3], [4], for non-dispersive channels [5] or for unamplified links with up to 1.2 dB of optical signal-to-noise ratio (SNR) gain with respect to standard QAM [6].

The channel model can be considered a layer in the deep neural network represented by the AE. A key requirement for classical gradient based optimization of an AE is then that the channel model is *differentiable*. This requirement is often too strict because 1) not all channel models are differentiable; 2) approximating a channel with a simple differentiable model results in inaccuracies [7]; 3) an accurate differentiable channel model can be too complicated for reliable optimization.

O. Jovanovic, M. Yankov, F. Da Ros, and D. Zibar are with the Department of Photonic Engineering, Technical University of Denmark, 2800 Kgs. Lyngby, Denmark, e-mail: ognjo@fotonik.dtu.dk

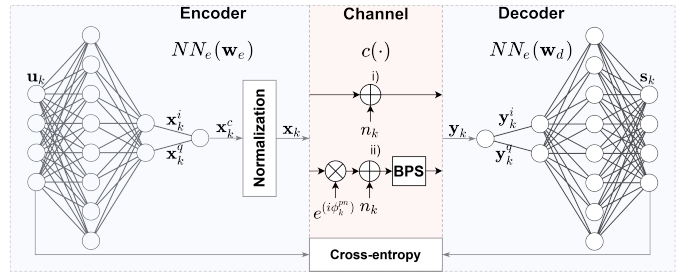


Fig. 1. Autoencoder model for geometrical constellation shaping. Channel models consist of: i) additive white Gaussian noise; ii) phase noise, AWGN and blind phase search algorithm for phase recovery.

The discrepancy between the channel model and the physical system can be avoided by using a generative adversarial network (GAN) as demonstrated in [8] for wireless communication and [7] for non-coherent fiber optic communication. However, the GANs require pre-training with experimentally obtained data, as well as re-training with newly generated experimental data after each AE optimization step, which can be time-consuming [7].

In this paper, the differentiable channel model requirement is lifted by proposing a derivative-free optimization method for AEs. This allows the AE to be optimized for arbitrary black-box channels, including non-numerical ones (e.g. experimental test-beds). The proposed method is exemplified by adopting the cubature Kalman filter (CKF) [9] for the optimization of an AE. The AE then performs GCS for a differentiable AWGN channel, resulting in nearly-identical performance to backpropagation, and then a phase noise channel with residual phase noise, resulting from a non-differentiable carrier phase recovery algorithm.

II. TRAINING OF AUTOENCODERS USING BAYESIAN FILTERING

The considered communication system employing an AE for geometrical constellation shaping is shown in Fig. 1. The encoder and the decoder are both represented by neural networks $NN_e(\mathbf{w}_e)$ and $NN_d(\mathbf{w}_d)$, parameterized with trainable weights $\mathbf{w}_e \in \mathbb{R}^n$ and $\mathbf{w}_d \in \mathbb{R}^m$, respectively. The aforementioned weight vectors are column vectors constructed by stacking the weights associated each neuron, started with the first neuron in the first hidden layer and progressing first in width (next neuron) and then in depth (next layer). The overall goal is to find the corresponding $NN_e(\mathbf{w}_e)$ and $NN_d(\mathbf{w}_d)$ topologies and the weight vector set, $\{\mathbf{w}_e, \mathbf{w}_d\}$, that

would maximize the mutual information (MI) of the channel under the consideration. More specifically, the goal of the encoder is to learn a geometrically shaped constellation that is robust to channel impairments, whereas the decoder learns to reconstruct the transmitted symbols with high fidelity.

The encoder ($NN_e(\mathbf{w}_e)$) performs a mapping of the input one-hot encoded vector $\mathbf{u}_k \in \mathbb{R}^M$ to an output vector $\mathbf{x}_k \in \mathbb{R}^2$, representing a point in a constellation plane, i.e. $[x_k^i, x_k^q]^T$. M is the number of constellation points, k is a running index and T denotes a transpose operator. The complex symbols are then formed and normalized to an average power of 1, and applied to the channel, see Fig. 1.

In this paper, we consider one sample per symbol channel model that contains phase noise and additive white Gaussian noise (AWGN). The phase noise ϕ_k^{pn} is modeled as a Wiener process with variance $\sigma_\phi^2 = 2\pi\Delta\nu T_s$. $\Delta\nu$ is the combined laser linewidth, and T_s is the symbol period. The AWGN term is characterized by noise power σ_N^2 .

The phase noise compensation is performed by a Blind Phase Search (BPS) algorithm which constitutes a non-differentiable part of the autoencoder [10]. The origin of the aforementioned non-differentiability is the hard-decision part of the algorithm associated with the symbol assignment. The output of the BPS, denoted by y_k is then applied the decoder neural-network $NN_d(\mathbf{w}_d)$ which uses softmax output layer to output a vector of posterior probabilities $\mathbf{s} \in \mathbb{R}^M$.

The AE structure depicted in Fig. 1 can be described using the state-space modelling framework. Then, given a data-set $\mathcal{D}_k = \{\mathbf{u}_k, K = 1, 2, \dots, K\}$, Bayesian filtering techniques can be applied to estimate \mathbf{w}_e and \mathbf{w}_d [11].

A. State-space model

In general, the state-space model is described by an equation describing the evolution of the states (non-observable variables that we would like to estimate) and the corresponding measurement equation that relates observable variables (\mathbf{s}_k for the considered case) with the states [11]. For the AE, the weights associated with the encoder and decoder neural-networks are considered as states and their evolution is described by the first-order auto-regressive equation:

$$\mathbf{w}_k = \mathbf{w}_{k-1} + \mathbf{q}_{k-1} \quad (1)$$

where $\mathbf{w}_k = [\mathbf{w}_{e,k}^T, \mathbf{w}_{d,k}^T]^T$ and \mathbf{q}_k represents process-noise term which corresponds to white Gaussian noise of zero mean and covariance matrix \mathbf{Q} . The process-noise term is intentionally included to avoid the states being trapped in a local minima during the initial training stage.

The measurement equation for the state-space model describing the AE needs to be adapted as the weight estimation \mathbf{w}_k is obtained by minimizing cross-entropy cost function for an M -class pattern-classification problem, and not the sum of squared errors as is typically the case. Minimizing the cross-entropy cost function is equivalent to maximizing mutual information (MI) between the transmitted and received symbol. The MI represents maximum achievable rate for given decoder. For the AE, the cross-entropy cost function is expressed as:

$$J_k = - \sum_{i=1}^M u_k^{(i)} \log \mathbf{h}^{(i)}(\mathbf{w}_{e,k}, \mathbf{w}_{d,k}, \mathbf{u}_k) \quad (2)$$

where $\mathbf{h}^{(i)}(\cdot)$ is an i th output of the decoder neural-network NN_d and accounts for the propagation through the encoder neural network, the phase noise channel model, the BPS phase compensation algorithm and the decoder neural network. Following the approach outlined in [11], the measurement equation is expressed as:

$$0 = \sqrt{J_k} + r_k \quad (3)$$

where r_k denotes measurement noise of zero mean and variance σ_r^2 which is related to the noise power added by the channel. The weight estimation within the state-space model given by equations (1) and (3) can be solved by using various nonlinear Bayesian state estimation techniques [11]. In this paper, we focus on using Cubature Kalman Filter (CKF) [9]. The advantage of using CKF is its accuracy and most importantly that it does not require computations of gradients providing a gradient-free training of AEs.

III. NUMERICAL RESULTS

In this paper, the AE architecture is a result of a coarse optimization. The encoder neural network has no hidden layers and all biases are set to zero, meaning the encoder actually performs linear mapping. The decoder neural network has a single hidden layer of $\frac{M}{2}$ nodes and *Leaky Relu* as the activation function. The system symbolrate is $R_s = 32$ GBd and the size of the constellation is $M = 64$. At each training iteration k , a batch of $B = 32 \cdot M$ one-hot encoded input vectors \mathbf{u}_k is generated. The hyperparameters of the CKF algorithm \mathbf{Q} and σ_r^2 are optimized using the grid search method. The training was done for each SNR value. The AE is trained until the cost function converges. Afterwards, the weights of the AE are fixed and testing is performed. The testing was done by running 100 simulations with 10^5 symbols per simulation. Each of the trained AE was tested with the same channel parameters as it was trained.

The constellations learned by AE will be compared to iterative polar modulation (IPM) [12] and square QAM (referred to simply as QAM in the following). The IPM was chosen as a benchmark because it is a near optimal constellation shape for the AWGN channel. It should be emphasised that in order to have a fair comparison between all the constellations, a mismatched Gaussian receiver [13] is used instead of the decoder neural network for the MI estimation, during the testing phase.

A. AWGN channel

An AE model that embeds the AWGN channel is shown in Fig. 1, *channel model i*). The noise variance is determined by the signal-to-noise ratio (SNR): $\sigma_N^2 = \frac{1}{SNR}$. The training of AE is performed for each of the SNR values in the interval $SNR = \{10, 11, \dots, 25\}$ dB.

As the AWGN channel model is differentiable, the comparison in the performance of the AE trained using the CKF and

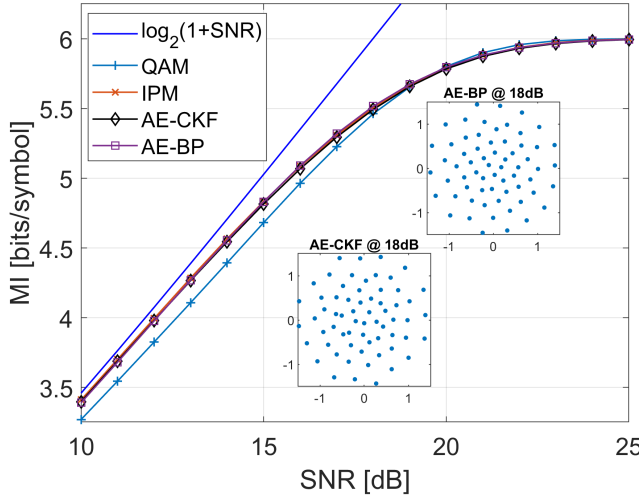


Fig. 2. AWGN channel: Mutual information as a function of SNR for constellation size $M = 64$.

the gradient based methods can be obtained. For the considered case, we employ backpropagation algorithm using the Adam optimizer as benchmark gradient based training method [14].

The simulation results of the testing for the AWGN channel are shown in Fig. 2, which illustrates the performance in MI with respect to the SNR. The learned constellations using the AE with trained with the CKF and the backpropagation are denoted as AE-CKF and AE-BP, respectively. This notation will be used throughout the rest of this section. The learned constellation AE-CKF and AE-BP result in a similar performance in the MI with an average difference of around 0.008 bits/symbol. Compared to QAM, the two constellations achieve higher MI for lower SNR, as expected, whereas the difference is marginal compared to the IPM. The insets illustrate the learned constellations AE-CKF and AE-BP when training on SNR = 18 dB.

The obtained results demonstrate that the proposed AE optimization method CKF can achieve similar performance to BP when the derivative of the channel model with respect to the encoder weights \mathbf{w}_e can be calculated.

B. Nondifferentiable phase noise channel

In this subsection, we consider a channel model for which the gradients cannot be computed. For this purpose, the phase noise channel with BPS phase noise compensation algorithm is considered, i.e. *channel model ii*) in Fig. 1.

The BPS is used as the phase recovery algorithm and it is the non-differentiable part of this channel model due to its hard-decision directed nature [10]. The BPS is a pure feedforward phase recovery algorithm based on rotating the received symbol by N_s test phases defined by:

$$\theta_i = \frac{i}{N_s} \cdot 2\pi, \quad i \in \{0, 1, \dots, N_s - 1\}. \quad (4)$$

Decisions are made on each of the rotated symbols and the distance between the decided symbol and the rotated symbol is calculated. Afterwards, distances of W consecutive symbols rotated by the same test phase are averaged over in order

to mitigate the effect of the AWGN on the quality of the decision. The optimal test phase is chosen by the minimum sum of distances [10]. The performance of the BPS algorithm is determined by the parameters N_s and W .

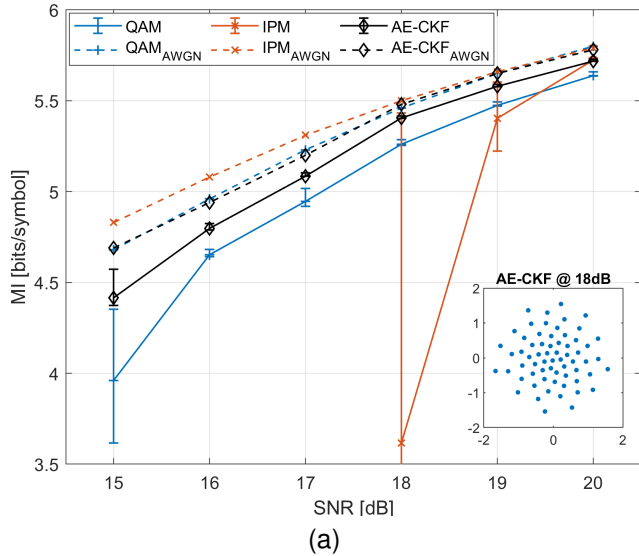
The of training of AE is performed for each of the SNR values in the interval $\text{SNR} = \{15, 16, \dots, 20\}$ dB combined with the BPS parameters $N_s = 36$ and $W = \{40, 64\}$ and linewidth $\Delta\nu = 100$ kHz.

In Fig. 3(a)-(b), the MI performance with respect to SNR is shown. The dashed lines show the performance of the constellations for AWGN channel. The dashed line $\text{AE-CKF}_{\text{AWGN}}$ presents the MI obtained when the AE-CKF trained for channel model ii) is tested on channel model i) for the respected SNR. The solid lines represent the average MI value over the 100 test simulations at a given SNR, whereas the upper limit of the error bar is the maximum obtained MI value and the lower is the 25th percentile. Therefore, the error bars represent the 75% of simulations with the highest MI.

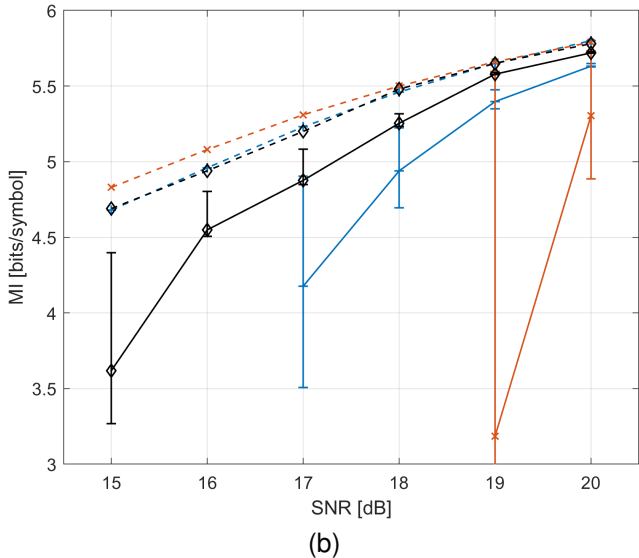
Fig. 3(a), shows MI with regards to SNR when the BPS parameters are $N_s = 36$ and $W = 64$. For the SNR values with a mean MI less than 3.5 bits/symbol, all points are removed from the figure for visual clarity. We would like to emphasize that the AE learned constellations achieve higher gain MI compared to QAM at $\text{SNR} = 15$ dB, and it amounts to around 0.45 bits/symbol. The gain in MI compared to QAM is 0.15 bits/symbol at $\text{SNR} = 16$ dB and with the increase of SNR the gain is slowly decaying to 0.08 bits/symbol, which is achieved at $\text{SNR} = 20$ dB. Observing the width of the error bars, it can be noticed that the spread of MI performance is smaller for the AE learned constellation compared to QAM, especially for lower SNR values. It can also be noticed that the maximum achieved MI value of QAM is lower than 25th percentile of the AE learned constellation, implying that the AE learned constellation has a better performance at least in 75% of the test cases. The AE-CKF and IPM constellations achieve similar maximum MI at high SNR but the AE-CKF is more robust and has a significantly higher mean MI value, whereas at $\text{SNR} = 20$ dB the two constellation have marginal differences in MI. The inset illustrates the learned constellations AE-CKF when training on $\text{SNR} = 18$ dB.

Next, the potential improvement at lower BPS complexity is analyzed. The window size was decreased to $W = 40$ and the results are illustrated in Fig. 3(b). All of the SNR points with a mean MI less than 3 bits/symbol were removed from the figure for visual clarity. The gain in MI achieved by the learned constellation compared to QAM at $\text{SNR} = 20$ dB is similar to the one achieved in the previous scenario, whereas compared to IPM for the same $\text{SNR} = 20$ dB greater gain was achieved, reaching a value of around 0.41 bits/symbol. The achieved gain is increasing with the decrease of SNR. The gain at $\text{SNR} = 17$ dB already exceeds the highest gain achieved in the previous scenario, reaching gain of around 0.7 bits/symbol. Similarly to the previous scenario the error bars of the AE-CKF constellation are less spread than for QAM and IPM at the same SNR, indicating better robustness of the constellation.

Observing the dashed lines in Fig. 3 shows that the AE-CKF constellation learned by training on channel model ii) lost



(a)



(b)

Fig. 3. *Nondifferentiable phase noise channel:* Mutual information as a function of SNR for constellation size $M=64$. The parameters of the BPS are: (a) $N_s = 36$ and $W = 64$ and (b) $N_s = 36$ and $W = 40$. The line shows the mean value, whereas the upper limit of the error bar is the max value and the lower limit is the 25th percentile. Points that have a mean less than 3.5 and 3 bits/symbol are omitted from the figure (**top**) and (**bottom**) for visual clarity, respectively. Inset: example of the learned constellation at $\text{SNR} = 18$ dB, $N_s = 36$ and $W = 64$.

AWGN shaping gain compared to when it was trained directly on AWGN channel. The AE-CKF_{AWGN} and QAM_{AWGN} now have similar performance in MI, whereas the penalty in MI, comparing situations with and without phase noise, is significantly lower for AE-CKF than for QAM. Therefore, the AE-CKF constellation is more robust to phase noise at an expense of slight loss of AWGN shaping gain.

IV. CONCLUSION

We have proposed and numerically demonstrated a derivative-free method for training of autoencoders for geometrical constellation shaping. This is achieved by expressing the autoencoder in a state-space model and then applying

cubature Kalman filter (CKF) for state (encoder and decoder weights) estimation. For a differentiable AWGN channel model, it was shown that the performance, in terms of the mutual information of the learned constellations, is almost identical to when the training is performed using the standard backpropagation algorithm. The CKF trained autoencoder was also tested for a phase noise channel with a non-differentiable phase recovery algorithm. In such a case, the autoencoder learned constellations achieved significant performance and robustness improvement with respect to conventional constellation shapes optimized for an AWGN channel.

ACKNOWLEDGMENT

This work was financially supported by the European Research Council through the ERC-CoG FRECOM project (grant agreement no. 771878), the Villum Young Investigator OPTIC-AI project (grant no. 29334), and DNRF SPOC, DNRF123.

REFERENCES

- [1] R. Essiambre, G. Kramer, P. J. Winzer, G. J. Foschini, and B. Goebel, “Capacity limits of optical fiber networks,” *Journal of Lightwave Technology*, vol. 28, no. 4, pp. 662–701, 2010.
- [2] T. O’Shea and J. Hoydis, “An Introduction to Deep Learning for the Physical Layer,” *IEEE Transactions on Cognitive Communications and Networking*, vol. 3, no. 4, pp. 563–575, 2017.
- [3] R. T. Jones, T. A. Eriksson, M. P. Yankov, and D. Zibar, “Deep Learning of Geometric Constellation Shaping Including Fiber Nonlinearities,” *European Conference on Optical Communication, ECOC*, 2018.
- [4] R. T. Jones, M. P. Yankov, and D. Zibar, “End-to-end learning for gmi optimized geometric constellation shape,” in *European Conference on Optical Communication, ECOC*, 2019.
- [5] S. Li, C. Häger, N. Garcia, and H. Wymeersch, “Achievable Information Rates for Nonlinear Fiber Communication via End-to-end Autoencoder Learning,” *European Conference on Optical Communication, ECOC*, 2018.
- [6] M. Schaedler, S. Calabro, F. Pittalà, G. Böcherer, M. Kuschnerov, C. Bluem, and S. Pachnicke, “Neural network assisted geometric shaping for 800Gbit/s and 1Tbit/s optical transmission,” *2020 Optical Fiber Communications Conference and Exhibition (OFC)*, vol. Part F174, no. DM, pp. 3–5, 2020.
- [7] B. Karanov, M. Chagnon, V. Aref, D. Lavery, P. Bayvel, and L. Schmalen, “Concept and experimental demonstration of optical im/dd end-to-end system optimization using a generative model,” *2020 Optical Fiber Communications Conference and Exhibition (OFC)*, pp. 1–3, 2020.
- [8] H. Ye, G. Y. Li, B.-H. F. Juang, and K. Sivanesan, “Channel agnostic end-to-end learning based communication systems with conditional gan,” in *2018 IEEE Globecom Workshops (GC Wkshps)*. IEEE, 2018, pp. 1–5.
- [9] S. Haykin and I. Arasaratnam, “Cubature kalman filters,” *IEEE Trans. Autom. Control*, vol. 54, no. 6, pp. 1254–1269, 2009.
- [10] T. Pfau, S. Hoffmann, and R. Noé, “Hardware-efficient coherent digital receiver concept with feedforward carrier recovery for M-QAM constellations,” *Journal of Lightwave Technology*, vol. 27, no. 8, pp. 989–999, 2009.
- [11] I. Arasaratnam and S. Haykin, “Nonlinear bayesian filters for training recurrent neural networks,” in *Mexican International Conference on Artificial Intelligence*. Springer, 2008, pp. 12–33.
- [12] I. B. Djordjevic, H. G. Batshon, L. Xu, and T. Wang, “Coded polarization-multiplexed iterative polar modulation (pm-ipm) for beyond 400 gb/s serial optical transmission,” *Optical Fiber Communication Conference*, p. OMK2, 2010.
- [13] A. Lapidoth and S. S. Shitz, “On Information Rates for Mismatched Decoders,” *IEEE Transactions on Information Theory*, vol. 40, no. 6, pp. 1953–1967, 1994.
- [14] D. P. Kingma and J. Ba, “Adam: A method for stochastic optimization,” *arXiv preprint arXiv:1412.6980*, 2014.